Arbitrary Polynomial Chaos-Based Power System Dynamic Analysis with Correlated Uncertainties

Xingrui Li[a], Chengxi Liu[a,] *, Chenxu Wang[a], Federico Milano[b]

[a] *School of Electrical Engineering and Automation, Wuhan University, Wuhan, China*
[b] *School of Electrical and Electronic Engineering, University College Dublin, Dublin, Ireland*

Abstract

This paper proposes a novel method based on arbitrary Polynomial Chaos (aPC) to evaluate how parameter and variable uncertainty impacts on the dynamic response of power systems. The method defines a set of orthogonal polynomials that approximate the relationship between the sources of uncertainties, such as the power generation of renewable energy resources, and the system dynamic response. Measurement data can be directly utilized to construct the aPC model without any prior knowledge of the probability distribution of the uncertainty. A whitening transformation method is also integrated to decouple correlated data sets and thus avoid errors caused by distribution fitting. Finally, to avoid numerical issues common to polynomial chaos methods, the k-means++ clustering is embedded in the aPC. The accuracy and computational efficiency of the proposed method are validated through the WECC 3-machine 9-bus system and the NE 16-machine 68-bus system.
© 2017 Elsevier Inc. All rights reserved.
Keywords: Uncertainty quantification; power system dynamics; renewable energy sources; arbitrary polynomial chaos; whitening transformation; k-means++ clustering.

1. Introduction

1.1. Motivations

The penetration of renewable energy sources (RES) has introduced a considerable level of uncertainty into power systems, which may negatively impact on their operation and security as well as complicate their steady-state and dynamic analyses [1-4]. In this paper, we focus on the study of the propagation of uncertainty caused by RES in the short-term dynamic response of power systems.

1.2. Literature Review

Several works have been presented in the literature to quantify the effect of uncertainty on power system dynamics. These fall into the following four main categories: (i) sampling methods, (ii) perturbation methods, (iii) optimization methods, and (iv) surrogate model methods.

Typical sampling methods that consider uncertainty in the initial value and in the parameters include Monte Carlo

* Corresponding author.
E-mail address: liuchengxi@whu.edu.cn
http://dx.doi.org/10.1016/j.ijepes.2021.00.000
0142-0615 /© 2021 Elsevier Inc. All rights reserved.

http://dx.doi.org/10.1016/j.ijepes.2021.000000

simulation (MCS). Another class of works that falls in the category of MCS methods considers time-varying stochastic noise modelled through stochastic processes and stochastic differential equations. Relevant works in this fields are, for example, [5, 6]. MCS are widely used as benchmarks due to their high accuracy. Nevertheless, the excessive computational burden of solving a huge number of simulations hinders their application in practical system analysis, especially for online simulations. To alleviate the above limitation from the perspective of sampling method, some advanced sampling methods are proposed and an important branch of which is variance reduction technique. Variance reduction techniques endeavor to devise an estimator that is asymptotically unbiased and exhibits smaller variance compared to MCS. The primary objective is to attain a specified level of precision by utilizing fewer samples, thereby enhancing the efficiency of the estimation process. Importance sampling, stratified sampling, and quasi-Monte Carlo are three common variance reduction techniques. Importance sampling determines an alternative and proper probability density function, also known as importance sampling density, and samples from it to reduce the estimator variance. It is efficient when direct sampling from the original distribution is challenging. In [7], an improved sequential importance sampling method is proposed to accelerate the computation of power system reliability assessment. Stratified sampling divides the variable space into non-overlapping strata and then samples are drawn from each stratum separately. Latin hypercube sampling [8] and Latin supercube sampling [9], which are typical stratified sampling techniques, are implemented to solve probabilistic load flow problems. In quasi-Monte Carlo method, samples are drawn by using deterministic, low-discrepancy sequences instead of random samples as MCS. In [10], Sobol sequence is employed to reduce computational burden of solving probabilistic optimal power flow problems.

Perturbation methods have a smaller computational burden than MCS and consist in observing the uncertain response under small perturbations around the equilibrium point based on simplified models, e.g., linearized models [11, 12]. However, a major limitation of perturbation methods is that their accuracy deteriorates when the system trajectories deviate significantly from the initial point due to the nonlinearity of the DAEs.

Optimization methods evaluate the systems security assessment under uncertainties with respect to given constraints by constructing uncertain optimization mathematical model [13, 14]. Nevertheless, the application in large scale systems is limited due to the excessive computational burden. Improvement of the methods or application of faster solution methods are to be further researched.

To deal with the issues above, surrogate-model methods build the nonlinear relationship between state response and uncertainties in specific forms. In [15], the state trajectories are constructed by a second-order Taylor-series approximation of the uncertain inputs. In [16], a third-order normal forms approximation is used to quantify inherent interactions of the system. However, the higher-order approximation and the higher the number of uncertain inputs, the higher computational burden of these trajectory-sensitive analysis methods. In [17], Kriging method is exploited to reduce the computational burden of optimal power flow. Nevertheless, Kriging is sensitive to outliers in the data, which may lead to biased predictions. In [18], Koopman operator-based surrogate model is built to capture the power system dynamic response under parameter uncertainty. But the performance of higher-order moments requires further research. Similarly, machine learning (ML) methods require a large amount of data [19], and the training process to construct the surrogate model is generally highly time-consuming.

Polynomial chaos expansion (PCE), which is a method for approximating the uncertain behavior of a complex system through a polynomial expansion of the input variables, is another subclass of surrogate model methods. PCE is popular in both mathematic and engineering fields [20-22]. The most significant advantage of PCE with respect to ML is that the former does not require an offline training procedure. Also, PCE adapts better to multidimensional random variables than trajectory-sensitive analysis methods. PCE can accurately and efficiently quantify the RES uncertainties by analytically constructing the relationship between random inputs and corresponding outputs using a set of orthogonal polynomials.

A commonly used PCE method is stochastic Galerkin method (SGM). It can achieve high accuracy because it ensures that the residue of the uncertain DAEs is orthogonal to the linear space spanned by the polynomial basis [23]. In [24], SGM is implemented to power system transient analysis and obtain high accuracy results due to the mathematically rigorous Galerkin projection process. However, new power system models based on Galerkin projection need to be derived mathematically and thus it requires to rewrite the code of original models, which is hard to be implemented in commercial software. Moreover, the number of equations after the projection increases

significantly with the number of random inputs and the state variables, and so does the computational burden.

An alternative class of PCE methods, namely probabilistic collocation method (PCM), only requires the input and output information of the power system and hence can be directly utilized in the mature simulation platform. PCM starts by generating a set of representative collocation points and then solve the polynomial coefficients using several methods, such as the regression method [25], interpolation method [6], and pseudo-spectral method [26]. In [27], roots of one higher-order univariate polynomial are used as interpolation points and the performance of PCM with its variant in short- and long-term dynamic simulation is discussed. In [28, 29], correlations of uncertain inputs are taken into consideration and Copula-based methods are utilized to eliminate their dependence.

Most PCM techniques require the knowledge of the distribution of random variables, to either modeling the uncertainties [27, 28], or the decorrelation process [29]. However, a precise knowledge of the distribution may not be realistic in practice. Hence, system operators and market participants often use probabilistic forecast techniques to obtain the distribution of stochastic processes, e.g., the output power of a wind power plant, in the future. These estimated distributions are then utilized, for example, for system dynamic security assessment (DSA) [30], storage system arrangement [31], and bidding strategy selection [32]. However, this approach has several limitations. First, if the size of available data is limited, especially for online DSA, the estimation of the distribution and probability density can be affected by large errors. Then, in practice the parameters of the distribution can change for different time scales [33]. For example, the Cauchy distribution is usually assumed for ultra-short-term (1min ~ 60min) [34] whereas Beta or Gaussian distributions usually fit better short-term (1h ~ 48h) forecasts [35]. Finally, analytical distribution functions not always fit well available data [36]. On the other hand, the proposed method relies on data and is thus exempt from the parameter forecast issues discussed above.

Admittedly, some non-parametric distribution fitting techniques, such as the kernel density estimation, that can be applied to obtain relatively accurate distribution information from measurement data. But these techniques generally constitute a numerical challenge for the construction of the orthogonal bases and cannot be effectively applied with limited raw data. Moreover, if a correlation exists among the raw data, it is difficult to find the appropriate joint probability density function which can precisely express the inherent correlation. And, even if known, the correlation can change depending on the time, day, season, and other exogenous factors.

1.3. Contributions

We propose a method to quantify the effect of uncertainty on the dynamic response of power systems based on the aPC structure. Specific contributions are as follows.

- The proposed algorithm directly utilizes raw data without any assumptions on the data distribution. This avoids errors given raise by casting samples into probability density functions and allows exploiting parallel computing to construct the polynomial basis.
- Whitening transformation is integrated with the aPC-based structure as preprocessing to tackle the correlation of uncertainties.
- K-means++ clustering method is adopted to find the collocation points. This avoids the problem of matrix singularity when attempting different combinations of roots.

1.4. Organization

The remainder of the paper is organized as follows. Section II describes the theoretical background of the polynomial chaos expansion and its coefficients calculation methods. Section III describes the proposed aPC-based uncertainty quantification framework in power system dynamics. Section IV discusses two case studies that verify the accuracy and efficiency of the proposed method. Finally, conclusions are drawn in Section V.

2. Theoretical Background

2.1. Surrogate Model Based on Polynomial Chaos Expansion

Let a vector of system response x be an implicit function $f(\xi)$ of multi-dimensional random variables ξ with cumulative distribution function $\Gamma(\xi)$ and space Ω:

$$x = f\left(\xi\right) \tag{1}$$

The advantage of the polynomial chaos expansion (PCE) method is that only a small number of simulations are required to extract the probability features of system outputs x. The outputs x are represented by a series of orthogonal polynomials and coefficients as follows [26]:

$$x = \sum_{i=0}^{N_p} a_i \varphi_i\left(\xi\right) \tag{2}$$

where x is a system output, such as a state variable of a generator or a bus voltage magnitude or angle; $\xi \in \mathbb{R}^N$ is a vector of multi-dimensional random inputs; a_i is the ith polynomial coefficient; φ_i is the ith term polynomial basis; $N_p=(N+d)!/(N!d!)-1$; d is the maximum order of univariate polynomial basis. The total number of simulations required is (N_p+1) which is the same as the number of polynomial coefficients to be determined. The basis $\{\varphi_j(\xi)\}$ for the multi-dimensional variables is constructed as:

$$\left\{\varphi_j\left(\xi\right)\right\} = \left\{\varphi_{j_1}\left(\xi_1\right)\varphi_{j_2}\left(\xi_2\right)\cdots\varphi_{j_N}\left(\xi_N\right), j_1 + j_2 + \cdots + j_N \le d\right\} \tag{3}$$

where $\varphi_{j_i}(\xi_i)$ denotes the j_ith order polynomial basis of the ith random variable. Taking the second-order expansion of two random variables as an example (N=2, d=2), the basis (3) is $\{1, \varphi_1(\xi_1), \varphi_1(\xi_2), \varphi_2(\xi_1), \varphi_2(\xi_2), \varphi_1(\xi_1)\varphi_1(\xi_2)\}$ and the size is (N_p+1)=6.

Random variables with different distributions have unique optimal polynomials which significantly affect the approximation accuracy of the surrogate model (2). If the random variables follow standard distributions, we can refer to the Wiener-Askey scheme to find the corresponding optimal orthogonal polynomials, such as for standard uniform and Gaussian distribution, the optimal polynomials are the Legendre and Hermite polynomials respectively. As for non-standard distribution, the Gram-Schmidt orthogonalization [37] or the Stieltjes procedure [27] can be applied to generate orthogonal polynomials. Both are based on the probability density function (PDF). This class of PCE that is based on the explicit forms of PDF is known as generalized polynomial chaos (gPC) [26].

2.2. Probabilistic collocation method

After optimal orthogonal polynomials are generated, either PCM or SGM can be applied to calculate the coefficients $\{a_i\}$ in (2). PCM is nonintrusive which means it can be implemented directly in commercial software, while SGM is intrusive that the built-in models need to be modified according to different simulation scenarios. Since the nonintrusive method has the advantages of easier application and more reliable performance, PCM is used in this paper.

Collocation points ξ_c are a set of samples of the random input variables. Traditionally, the combinations of roots of one higher-order univariate polynomial are usually chosen as collocation points, which is also known as the root method [26]. The number of collocation points exactly equals the number of multi-dimensional bases (N_p+1) and the corresponding response $\{x_c\}$ of collocation points is simulated. Then, the coefficients $\{a_i\}$ can be computed by solving the linear equation below:

$$\begin{bmatrix} a_0 \\ a_1 \\ \vdots \\ a_{N_P} \end{bmatrix} = \begin{bmatrix} \varphi_0\left(\xi_{c_1}\right) & \varphi_1\left(\xi_{c_1}\right) & \cdots & \varphi_{N_P}\left(\xi_{c_1}\right) \\ \varphi_0\left(\xi_{c_2}\right) & \varphi_1\left(\xi_{c_2}\right) & \cdots & \varphi_{N_P}\left(\xi_{c_2}\right) \\ \vdots & \vdots & \vdots & \vdots \\ \varphi_0\left(\xi_{c_{N_P+1}}\right) & \varphi_1\left(\xi_{c_{N_P+1}}\right) & \cdots & \varphi_{N_P}\left(\xi_{c_{N_P+1}}\right) \end{bmatrix}^{-1} \begin{bmatrix} x_{c_1} \\ x_{c_2} \\ \vdots \\ x_{c_{N_P+1}} \end{bmatrix} \tag{4}$$

Or in vector form:

$$a = H_\varphi^{-1} x \tag{5}$$

It indicates that the surrogate model (2) only requires the form of orthogonal polynomials, the pre-selected collocation points, and the corresponding response of the given model in advance.

2.3. Post-Processing for statistical characteristics

Orthogonality is an important property that polynomials must satisfy which provides convenience in extracting the probabilistic features of the system outputs. Orthogonality of two polynomials $\varphi_{k_1}(\xi_i)$ and $\varphi_{k_2}(\xi_i)$ is defined as below:

$$\begin{aligned} \left\langle \varphi_{k_1}\left(\xi_i\right), \varphi_{k_2}\left(\xi_i\right) \right\rangle &= \int_{\xi_i \in \Omega} \varphi_{k_1}\left(\xi_i\right) \varphi_{k_2}\left(\xi_i\right) d\Gamma\left(\xi_i\right) \\ &= \delta_{k_1 k_2} \left\| \varphi_{k_1}\left(\xi_i\right) \right\|_2^2 \end{aligned} \tag{6}$$

where $\langle \cdot,\cdot \rangle$ is the inner product; $k_1,k_2=\{0,1,\ldots,d\}$; $\Gamma(\xi_i)$ is the cumulative distribution function of the ith random input ξ_i; $\|\cdot\|_2$ is the 2-norm; $\delta_{k_1 k_2}$ is the Kronecker delta function.

Based on the orthogonality, we can directly obtain the expectation and variance of the output x in (2) according to the coefficients $\{a_i\}$ as:

$$\begin{aligned} \mu_x &= \int_{\xi \in \Omega} f\left(\xi\right) d\Gamma\left(\xi\right) = a_0 \\ \sigma_x^2 &= \int_{\xi \in \Omega} \left(f\left(\xi\right) - \mu_x\right)^2 d\Gamma\left(\xi\right) = \sum_{i=1}^{N_p} a_i^2 \left\| \varphi_i\left(\xi\right) \right\|_2^2 \end{aligned} \tag{7}$$

The analytical expressions of high-order moments, such as skewness and kurtosis, can also be derived based on the coefficients $\{a_i\}$ and (7).

Thus, by only performing (N_p+1) simulations, moments of outputs are easily obtained from the coefficients. Note that since the PCE model is analytical at every moment, the statistical information, e.g., mean, variance, and probability distribution, can also be cheaply obtained by MCS.

3. Proposed Arbitrary Polynomial Chaos Framework in Power System Dynamics

3.1. Modeling Parametric Uncertainties in Power System Dynamics

Traditionally, the uncertainties of the RES in dynamic power systems are not considered, which means they are treated as constants instead of variables. The dynamic model of power systems with uncertain inputs can be expressed by the following DAE:

$$\begin{cases} \dot{x} = f(x, y; \xi) \\ 0 = g(x, y; \xi) \end{cases} \tag{8}$$

where $x \in \mathbb{R}^n$ is the vector of state variables, such as rotor angles and rotor speeds; $y \in \mathbb{R}^m$ is the vector of algebraic variables, such as bus voltage magnitudes and angles; $\xi \in \mathbb{R}^N$ is the vector of uncertain variables we are interested in, such as power injections of RES; $f(\cdot)$: $\mathbb{R}^n \times \mathbb{R}^m \times \mathbb{R}^N \to \mathbb{R}^n$ and $g(\cdot)$: $\mathbb{R}^n \times \mathbb{R}^m \times \mathbb{R}^N \to \mathbb{R}^m$ are the nonlinear implicit differential and algebraic equations, respectively. Note that, in this model, uncertainty is assumed to exist only at the beginning of the simulation and remains unchanged after the initial point.

3.2. Constructing Polynomial Basis of aPC

Unlike gPC, which requires to use detailed and explicit PDF, aPC directly utilizes the moments of raw data to build polynomial basis. We take one-dimensional random variable case as an example, the kth order polynomial basis $\varphi_k(\xi_i)$ for the ith random variable $\xi_i \in \xi$ is defined as below [38]:

$$\varphi_k(\xi_i) = \sum_{l=0}^{k} c_l^{(k)} (\xi_i)^l \tag{9}$$

where $k=\{0,1,\ldots,d\}$ is the degree of polynomial basis; $\{c_l^{(k)}\}$ are the unknown coefficients in $\varphi_k(\xi_i)$.

To more intuitively carry out further derivation, (6) can be represented as:

$$\int_{\xi_i \in \Omega} \varphi_{k_1}(\xi_i) \varphi_{k2}(\xi_i) d\Gamma(\xi_i) = \begin{cases} 0, & k_1 \neq k_2 \\ \left\| \varphi_{k_1}(\xi_i) \right\|_2^2, & k_1 = k_2 \end{cases} \tag{10}$$

Besides, we assume the leading coefficients of all polynomials to be 1:

$$c_k^{(k)} = 1, \quad \forall k \tag{11}$$

It is worth mentioning that (11) is not strictly necessary because there is always a set of following coefficients $\{c_l^{(k)}\}$ where $l=\{0,1,\ldots,k\text{-}1\}$ that makes the orthogonality of the whole set of polynomial bases satisfied. The condition (11) serves only to simplify the notation of following derivations.

If $k=0$, we can obtain directly from (11) that $\varphi_0 = c_0^{(0)} = 1$. Then, the following relation of coefficients based on (10) can be obtained:

$$\begin{aligned} &\int_{\xi_i \in \Omega} c_0^{(0)} \left[\sum_{l=0}^{k} c_l^{(k)} (\xi_i)^l \right] d\Gamma(\xi_i) = 0 \\ &\int_{\xi_i \in \Omega} \left[\sum_{l=0}^{1} c_l^{(1)} (\xi_i)^l \right] \left[\sum_{l=0}^{k} c_l^{(k)} (\xi_i)^l \right] d\Gamma(\xi_i) = 0 \\ &\vdots \\ &\int_{\xi_i \in \Omega} \left[\sum_{l=0}^{k-1} c_l^{(k-1)} (\xi_i)^l \right] \left[\sum_{l=0}^{k} c_l^{(k)} (\xi_i)^l \right] d\Gamma(\xi_i) = 0 \end{aligned} \tag{12}$$

The orthogonality of the polynomial of degree k is presented by (12). Then we substitute (11) to the first equation of (12), we have:

$$\int_{\xi_i \in \Omega} \sum_{l=0}^{k} c_l^{(k)} \left(\xi_i\right)^l d\Gamma\left(\xi_i\right) = 0 \tag{13}$$

Next, we substitute (11) and (13) to the second equation of (12), we obtain:

$$\int_{\xi_i \in \Omega} \sum_{l=0}^{k} c_l^{(k)} \left(\xi_i\right)^{l+1} d\Gamma\left(\xi_i\right) = 0 \tag{14}$$

If we continue this procedure to the rest equations in (12), we can finally re-write (12) with the assumption (11) as follows:

$$\begin{aligned}
&\int_{\xi_i \in \Omega} \sum_{l=0}^{k} c_l^{(k)} \left(\xi_i\right)^l d\Gamma\left(\xi_i\right) = 0 \\
&\int_{\xi_i \in \Omega} \sum_{l=0}^{k} c_l^{(k)} \left(\xi_i\right)^{l+1} d\Gamma\left(\xi_i\right) = 0 \\
&\vdots \\
&\int_{\xi_i \in \Omega} \sum_{l=0}^{k} c_l^{(k)} \left(\xi_i\right)^{l+k-1} d\Gamma\left(\xi_i\right) = 0 \\
&c_k^{(k)} = 1
\end{aligned} \tag{15}$$

Note that for different degrees *k,* the corresponding set of orthogonal polynomials are independent to others, which means we can improve the computing speed by applying parallel computing techniques.

Then, to further simplify (15), we introduce the *k*-th raw moment μ_k of ξ_i which is defined as:

$$\mu_k = \int_{\xi_i \in \Omega} \left(\xi_i\right)^k d\Gamma\left(\xi_i\right) \tag{16}$$

So the sets of equations in (15) can be presented by the raw moments μ_k in the matrix form:

$$\begin{bmatrix} \mu_0 & \mu_1 & \cdots & \mu_k \\ \mu_1 & \mu_2 & \cdots & \mu_{k+1} \\ \vdots & \vdots & \vdots & \vdots \\ \mu_{k-1} & \mu_k & \cdots & \mu_{2k-1} \\ 0 & 0 & \cdots & 1 \end{bmatrix} \begin{bmatrix} c_0^{(k)} \\ c_1^{(k)} \\ \vdots \\ c_{k-1}^{(k)} \\ c_k^{(k)} \end{bmatrix} = \begin{bmatrix} 0 \\ 0 \\ \vdots \\ 0 \\ 1 \end{bmatrix} \tag{17}$$

where the *n*th raw moment μ_n of ξ_i, $n=\{1,2,\ldots,2k\text{-}1\}$ can be obtained from either the data set or PDF of ξ_i by:

$$\begin{aligned}
\mu_n &= \frac{1}{N_d} \sum_{j=1}^{N_d} \xi_{i,j}^n \\
&= \int_{\xi_i \in \Omega} \left(\xi_i\right)^k \rho\left(\xi_i\right) d\xi_i
\end{aligned} \tag{18}$$

where N_d is the size of the data set; $\xi_{i,j}$ is the *j*th sample point of ξ_i; $\rho(\xi_i)$ is the PDF of ξ_i.

As a result, all coefficients $c_l^{(k)}$, $l=\{0,1,\ldots,k\}$ for any *k*-th order polynomials can be obtained if the moments' matrix

in (17) is not singular. This condition is equivalent to two constraints: the number of data with unique values N_u is larger than k, and the moments up to (2k-1)th order exists and is finite (see proof in Appendix A). For the former constraint, N_u discussed in this paper, such as the measurement of power injections of RES, is usually at least more than dozens, while the maximum polynomial order d of the proposed method is generally within 5. For the latter one, all moments are always existed and finite if every sample in data sets is finite. Hence for a limited order d, the measurement data set of ξ_i always satisfies the conditions above. Note that (12) is an intermediate process needed to calculate the coefficients of the univariate polynomials and it is finally transformed into (17) which is the actual equation that we use to derive the polynomial coefficients. The number of random variables does not affect the complexity of process when constructing the basis, since we construct the optimal orthogonal polynomial basis for a single random variable and repeat this process to all random variables.

To utilize the important property of PCE (7), we further transform one-dimensional form of (7) into a moment-based form by combining (10) and PDF form of (18):

$$\begin{aligned}\mu_x &= E\left[\sum_{j=0}^{d} a_j \varphi_j\left(\xi_i\right)\right] \\ &= a_0 \mu_0 \\ \sigma_x^2 &= E\left[\left(\sum_{j=0}^{d} a_j \varphi_j\left(\xi_i\right)\right)^2\right] - E\left[\sum_{j=0}^{d} a_j \varphi_j\left(\xi_i\right)\right]^2 \\ &= \sum_{j=1}^{d} a_j^2 \sum_{u=0}^{j} \sum_{v=0}^{j} c_u c_v \mu_{u+v}\end{aligned} \tag{19}$$

where $E[\cdot]$is the expectation operator. From (17) to (19), it is observed that for a certain expansion order d, only the first 2d moments of ξ_i are required to construct the polynomial basis and obtain the mean and variance of the state variables. Also, if the first 2d-1 order moments of two different random variables are the same, they will share the same first d order polynomial basis. Furthermore, higher-order moments of x can be obtained using more moments of ξ_i, such as first 3d and 4d moments are required for skewness and kurtosis respectively. Multi-dimensional polynomial basis can be determined after the one-dimensional basis of each ξ_i is constructed as in (3). The corresponding multi-dimensional statistical results can be obtained similarly as in (19).

The biggest difference between aPC and gPC is that the input ξ_i of aPC can have an arbitrary form (including raw data), distribution or even only moments, whereas gPC requires the analytic form of PDF. This specific feature makes aPC particularly suited for engineering applications. Besides, to perform basis truncation and adaptation handling high-dimensional uncertainties in systems with strong nonlinearity, existing techniques, such as the Smolyak adaptive sparse algorithm [39], can be conveniently combined with the proposed aPC method. Since the proposed method aims to build the polynomial basis in a more precise way and it does not affect the adaptive process to incrementally add higher-order terms.

3.3. Selection of Collocation Points

Compared to MCS, only a small number of simulations are needed by aPC. But, to this aim, the selected collocation points should be representative. If the collocation points fail to describe the probabilistic characteristics of ξ_i, the final approximation results can be inaccurate. To find representative collocation points, the root method is usually implemented in PCM [26]. However, we found in the simulation cases of multi-dimensional random variables, although higher-order roots are representative theoretically, the polynomial matrix H_φ in (5) might be singular due to an invalid combination of roots. This makes (5) unsolvable and requires randomly retrying different root combinations. Therefore, it is of great significance to determine suitable collocation samples in the first place.

The k-means++ clustering method is implemented in the aPC structure to find representative collocation points (cluster centroids). In [40], the results of the effect of skewed data distribution on k-means clustering are provided and

the intrinsic characterization of the relationships between data distribution and k-means clustering is studied. This work helps to build the connection between the centroids of clusters and the data distribution. It is a typical partitional clustering technique that is widely implemented in solving multidimensional data sets problems. It attempts to find k nonoverlapping clusters and corresponding centroids which are chosen as collocation points in this paper.

In the k-means++ clustering method, after the first initial centroid is determined randomly from the data set, the following initial centroids will be chosen one by one according to the probability $P(x_i)$:

$$P(x_i) = \frac{d(x_i)^2}{\sum d(x_j)^2} \qquad i, j = 1, ..., n \tag{20}$$

where $x_i \in \mathbb{R}^N$ is the ith group of samples of all random variables; $d(\cdot)$ is the distance from the sample to the existing closest centroid; n is the size of the data sets.

Then in the following iterations, it aims to minimize the sum of Euclidean distance between each sample and their closest cluster centroid:

$$\arg\min \sum_{l=1}^{k} \sum_{x \in C_l} \|x - T_l\|^2 \tag{21}$$

where $x \in \mathbb{R}^{N \times n}$ is the input data sets of k-means++ clustering method; $T_l = \Sigma_{x \in C_l}(x/n_l)$ is the centroid of the l-th cluster C_l; n_l is the number of samples in C_l; k is the number of clusters.

The overall clustering procedure of k-means++ is as follows. First, k, which is predetermined, initial centroids are selected according to (20) except for the first one that is chosen randomly. Then all points are assigned to the clusters with a minimum distance to the centroid and the collection of points to the same centroid forms a cluster. The centroids are updated after every assignment. This procedure is repeated until no point is reassigned.

After the iteration converges, k cluster centroids are determined. The distribution of data points has a relationship with the corresponding centroids which represent the interior characteristics of clusters. So, by setting collocation points to cluster centroids, we can avoid the problem of matrix singularity.

3.4. Decorrelation of Uncertain Inputs

PCE-based time-domain simulation methods assume that the uncertain input variables are mutually independent. The main reason is that in the process of deriving (7) and (19), the joint probability density of multidimensional random variables can be decomposed directly to corresponding marginal PDF only when variables are independent. A considerable error could be introduced if there are correlations between the inputs. However, the truth is correlations are identified in practical engineering, such as power generation of neighboring solar or wind farms and load demands in the same region. Thus, this motivates us to conduct research on decorrelation methods.

There are mainly two ways to solve the problem above, which are both based on joint and marginal probability density. The first is to calculate the integral in (7) directly according to the fitted joint probability density. The second uses the Copula theory which is an effective approach to transforming correlated uncertain variables into an independent space. However, if the form of inputs is data set, the probability density fitting error may negatively impact the accuracy, especially when the historical dataset is small. To avoid this problem, we apply the whitening transformation technique to directly obtain the decorrelated data from the raw data.

Whitening transformation is utilized to handle dependent random variables, such as in [41]. It is used as a preprocessing step in the proposed aPC structure for its data-driven feature. Assume $\zeta \in \mathbb{R}^{N \times Nd}$ is the dataset of random variables that has been centered. The covariance matrix Σ is defined as:

$$\Sigma = \mathrm{cov}(\zeta) = E\left[\zeta \zeta^T\right] \tag{22}$$

We exploit the transposition of the lower triangular matrix L^T as a whitening matrix:

$$\zeta_d = L^T \zeta \tag{23}$$

where ζ_d are the decorrelated datasets; L is the lower triangular matrix in the Cholesky decomposition of Σ^{-1}.

One of the advantages of combining the whitening transformation technique with the proposed aPC-based structure is that the form of whitening transformation results is data set, which can be directly utilized in the following aPC process. Besides, instead of explicitly using PDF, whitening transformation can avoid fitting errors.

3.5. Overall Implementation Procedure

The overall procedure of the proposed aPC-based polynomial uncertainty quantification method for dynamic power systems is summarized in Fig. 1.

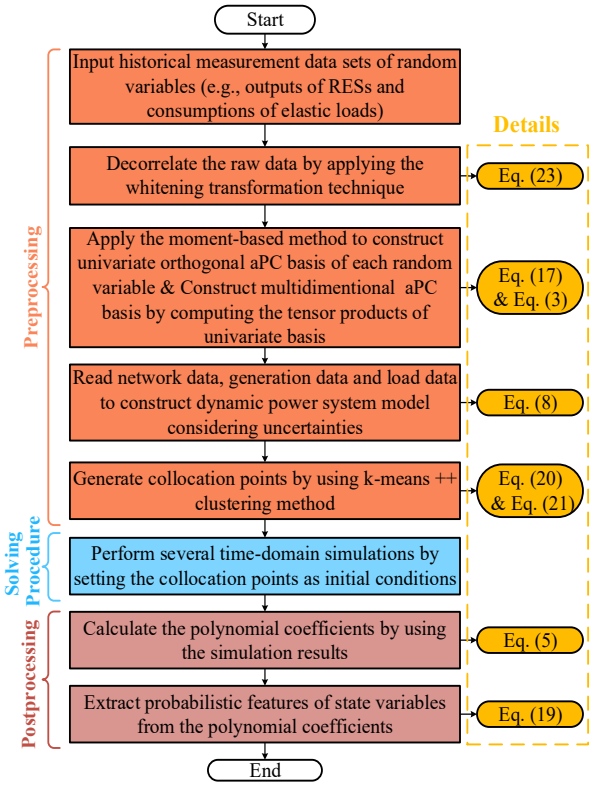

Fig. 1. Flowchart of the proposed uncertainty quantification method.

4. Case Studies

In this section, we apply the proposed aPC-based method in two benchmark power systems. The first case study includes two scenarios which are conducted on the modified Western Electricity Coordination Council (WECC) 3-machine 9-bus system with classical generator models [42]. The first scenario has only one random variable and serves to illustrate the features of the aPC method by comparing its accuracy and efficiency with the gPC and MCS methods. The second scenario has two linear correlated variables. We focus on the aPC algorithm performance with the combination of whitening transformation and k-means++ clustering method.

The second case study is conducted using real-world measurement data and a larger test system. The network is a modified model of the IEEE 69-machine 300-bus system with the detailed 6-order generator model, excitation, and

turbine system [42]. Nonlinear correlated photovoltaic (PV), wind generations and random loads are integrated into the system. This case demonstrates the robustness of the proposed method when applied to a larger system with various sources of uncertainty. Moreover, the second case study also serves to test the performance of the aPC under the assumption of nonlinear correlation among measurement data. The largest dimension of random inputs in this paper is set to 40 because this paper mainly focuses on the data-driven uncertainty quantification process rather than solving high-dimensional problems. The proposed algorithm in this paper can be integrated with any of the several state-of-the-art sparse PCE schemes to solve high-dimensional uncertainties, e.g., [43], but this is out of the scope of this manuscript.

By setting the results of MCS as the benchmark, the Average Absolute Error (AAE) e can be used as performance comparison index:

$$e = \frac{\sum_{i=1}^{N} \left| P_i - \hat{P}_i \right|}{N} \tag{24}$$

where P_i and $\hat{P}_i$ are the probabilistic characteristics (mean or standard deviation) of the state variable by using MCS and PCE in the ith timestep, respectively; N is the total number of simulation moments. Then, the computational burden is divided into preprocessing time t_{pre}, solving procedure time t_{sol}, postprocessing time t_{post}, as shown in Fig. 1.

All simulations have been carried out using Matlab R2016b on a laptop with Intel Core i5-10210U (4.2GHz) and 16GB RAM. The initial power flow results of the time-domain simulations are derived by MATPOWER 7.1 [44] and time-domain simulations are carried out based on PSDAT [45].

4.1. WECC 9-Bus System

1) Scenario 1: One Random Variable

In this first scenario, we assume that a wind farm is added in bus 3 to account for the uncertainty. The data power injection of the wind farm during a single day comes from the German Transmission System Operators (GTSO) [46]. A three-phase fault occurs at 1 second and is cleared by opening the line 8-9 after 0.1 second. The benchmark is obtained based on MCS, using the measurement data of one day that is measured every 15 minutes, a total of 96. Note that we have chosen to use a relatively short data set on purpose, in order to test a worst case scenario where the availability of raw data is limited, such as the case of online DSA. Simulation results reflect the superiority of aPC driven by data and the significant error introduced by gPC due to PDF fitting.

We observe the trajectories of the rotor angle δ_2 and the rotor speed ω_2 of generator 2. The orders of expansion for both aPC and gPC methods are set from 1 to 3. To avoid the interference of other conditions and only test the performance of different orthogonal basis construction processes between the aPC and gPC, the collocation points both are calculated based on the root methods [26]. The PDF used in gPC is fitted from the raw data and the orthogonal basis is constructed by the Gram-Schmidt orthogonalization method [37].

A quantitative AAE comparison of δ_2 and ω_2 is shown in Table 1**,** where the mean and standard deviation are represented by M. and S.D. The percentage number means the AAE of aPC as a percentage of the AAE of gPC. The results show that aPC has better accuracy than gPC in every order. Besides, with the order increase from 1 to 2, the accuracy of gPC is even worse, while the improvement of using aPC is significant. This is because for the gPC method, a considerable amount of error is introduced in the PDF fitting process which also impacts the precision of the orthogonal basis and the collocation points performance. Thus, though the order is increased, the approximation accuracy decreases in the end. This indicates that, in this scenario, increasing the order of gPC fails to improve the accuracy which poses the limitation of this method.

The problem above is avoided in the aPC method since it constructs the orthogonal basis purely from the original raw data instead of the fitted PDF and chooses collocation points based on accurate orthogonal basis. When the order increases to 3, the accuracy of mean of aPC remains almost the same to the second order, while the standard deviation can still be improved. This indicates that the upper bound of mean accuracy is reached while the standard deviation

still has room for improvement. In contrast, the performance of third order gPC gets worse than that of second order. Table 1 reflects the superiority of the proposed data-driven aPC method and at the same time, the significant error introduced by gPC due to PDF fitting.

The computational burden of PCE-based methods is compared with the MCS method in Table 2. Both gPC and aPC methods can significantly reduce computational burden while achieving comparable precision. Take the second order expansion as an example, only 3 time-domain simulations are required to extract the statistical information of the state variables instead of 96 in the MCS. Moreover, aPC can further shorten the time consumption to some extent in the preprocessing and postprocessing stage. For preprocessing stage, on the one hand, in the orthogonal basis construction process of aPC (17), parallel computing architecture can be deployed while only the serial calculation method is applicable to the Gram-Schmidt orthogonalization process of gPC. On the other hand, the integral operation of the Gram-Schmidt method is also more time-consuming than the linear equations solving process (17). For postprocessing stage, the integral operation of calculating the 2-norm in (7) is more complex than simply substitute moment information into (19).

The Mean, standard deviation error using second order gPC and aPC, and the bounds of aPC with MCS results of δ_2 and ω_2 are plotted in Fig. 2 and Fig. 3 respectively. Fig. 2.a, Fig. 2.b, Fig. 3.a and Fig. 3.b show that the initial points approximations of aPC are more accurate meanwhile the error fluctuation ranges are much smaller. Also, the maximum approximation error of aPC after the fault is cleared remains relatively stable while that of gPC deteriorates considerably. Moreover, the average absolute mean and S.D. error are increased along with time for both PC-based methods. The major reason is that a certain distribution of solution is assumed at the initial time, however, this may not fulfill the real shape or distribution after a long time which leads to a decrease in accuracy. Several methods are proposed to tackle this issue, such as multi-element [47] and time-dependent PC [48]. Besides, it is worth noticing that both gPC and aPC have some spikes during the fault. The reason is that if the approximated variables change too fast, or even step change occurs in some cases, the performance of both PCE-based methods decreases accordingly due to the limited order of expansion. The upper and lower bounds of aPC are given in Fig. 2.c and Fig. 3.c according to the 3σ rule [27]. These results not only intuitively reflect the uncertainty of the state variables caused by random power injection of wind farms but demonstrate the capability and accuracy advantage of aPC to estimate system uncertainty intervals, which provides operators with information to figure out how to reduce the system fluctuations.

Table 1
AAE of the rotor angle and rotor speed in different orders of gPC and aPC

Method	$e_{\delta 2}$(rad×10^{-5})		$e_{\omega 2}$(rad/s×10^{-3})	
	M.	S.D.	M.	S.D.
gPC (d=1)	112.02	288.56	20.18	50.56
aPC (d=1)	27.57(24.61%)	184.86(64.06%)	5.33(26.41%)	34.83(68.89%)
gPC (d=2)	182.20	994.72	31.26	169.75
aPC (d=2)	8.79(4.82%)	20.74(2.09%)	1.41(4.51%)	4.85(2.86%)
gPC (d=3)	197.20	1389.83	30.25	213.22
aPC (d=3)	9.07(4.60%)	7.67(0.55%)	1.41(4.66%)	1.30(0.61%)

Table 2
Computational burden of different orders using MCS, gPC and aPC

Order	Method	Time Components(s)			t_{total}(s)
		t_{pre}	t_{sp}	t_{post}	
-	MCS	-	973.24	0.01	973.25
1	gPC	1.67	22.14	4.65	28.46(2.92%)
	aPC	0.64	21.55	4.38	26.57(2.73%)
2	gPC	8.99	32.16	4.79	45.94(4.72%)
	aPC	0.64	33.41	4.91	38.96(4.00%)
3	gPC	10.76	40.80	4.58	56.14(5.77%)
	aPC	0.96	41.73	4.22	46.91(4.82%)

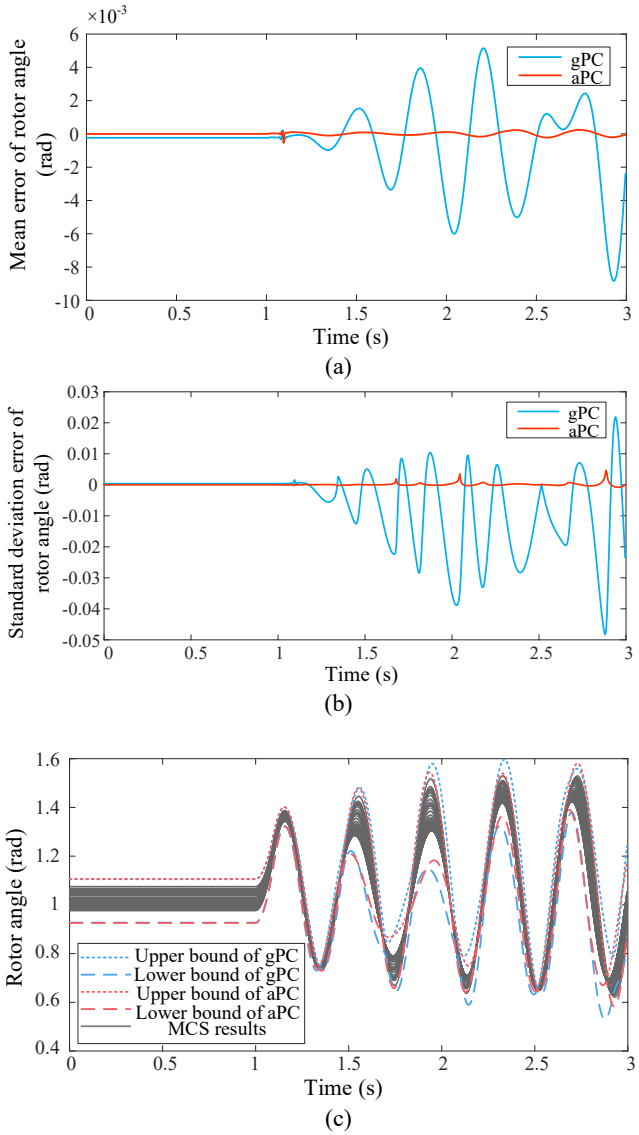

Fig. 2. Mean, standard deviation error of δ_2 using second order gPC and aPC methods and bounds using aPC method with MC results. (a) Average absolute mean error. (b) Average absolute variance error. (c) The upper and lower bounds of the gPC and aPC methods and MCS results.

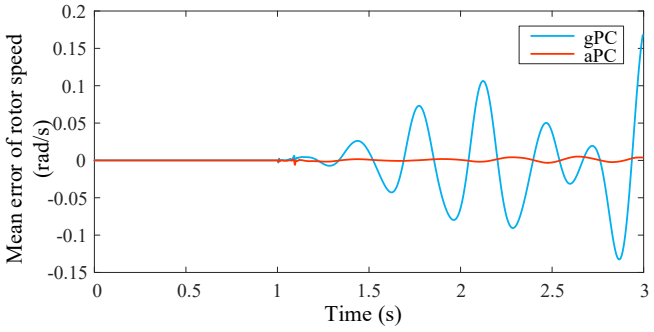

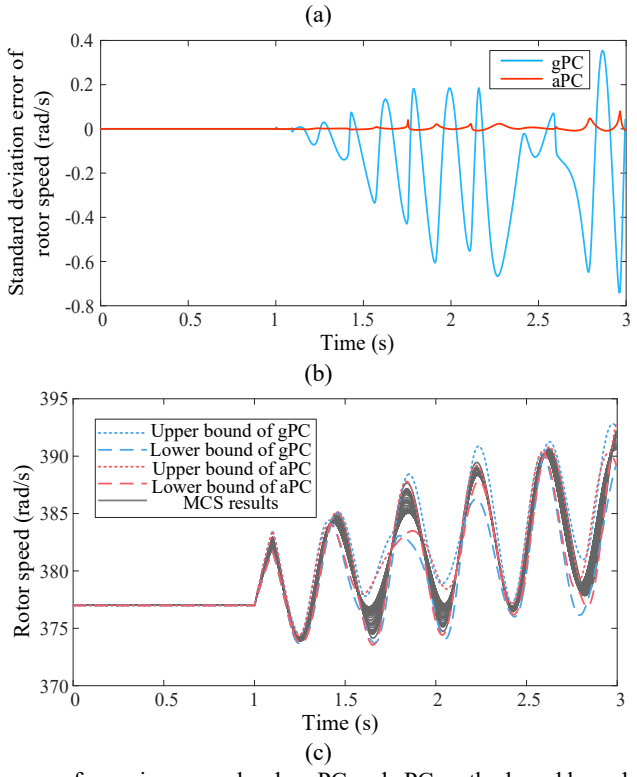

Fig. 3. Mean, standard deviation error of ω_2 using second order gPC and aPC methods and bounds using aPC method with MC results. (a) Average absolute mean error. (b) Average absolute variance error. (c) The upper and lower bounds of the gPC and aPC methods and MCS results.

Table 3
AAE of the rotor angle in different correlation coefficients

ρ	e_{δ_1}(rad×10^{-4})	gPC	aPC	
			k-means++ clustering	Root method
0.3	M.	198.75	9.68(4.87%)	9.65(4.86%)
	S.D.	54.35	44.79(82.41%)	44.70(82.24%)
0.6	M.	199.25	9.89(4.96%)	9.85(4.94%)
	S.D.	60.44	40.20(66.51%)	40.24(66.58%)
0.9	M.	198.12	9.48(4.78%)	9.49(4.79%)
	S.D.	69.81	35.98(51.54%)	35.93(51.47%)

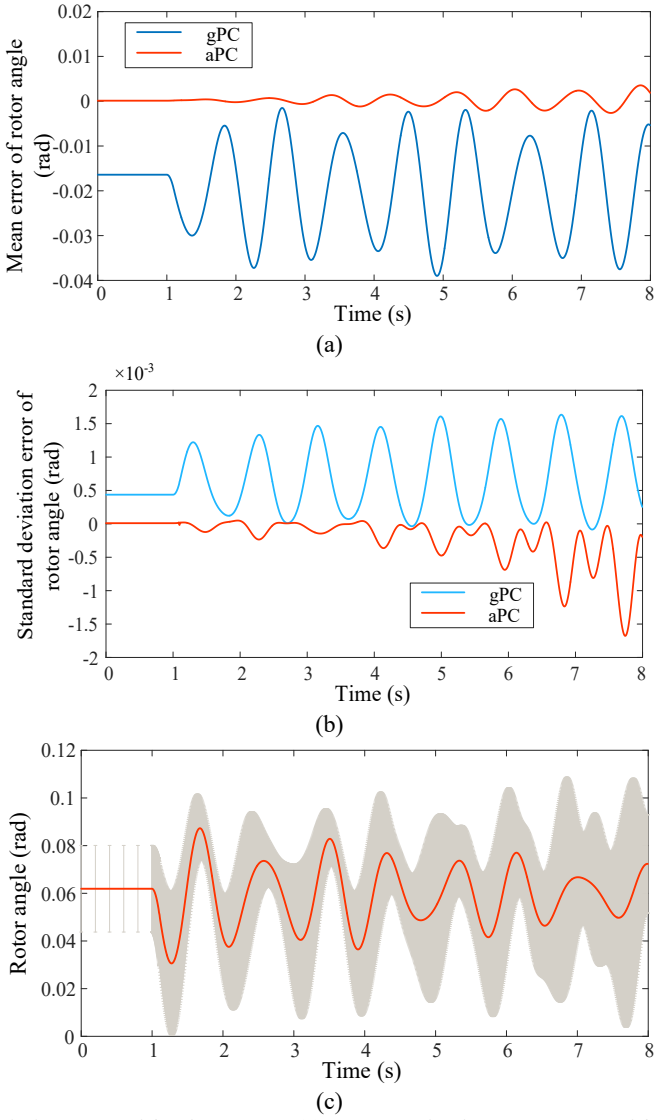

Fig. 4. Mean and standard deviation error of δ_1 when ρ=0.6. (a) Average absolute mean error of δ_1 using gPC, aPC methods. (b) Average absolute standard deviation error of δ_1. (c) Mean and error bar of δ_1 using aPC method.

2) Scenario 2: Two Correlated Random Variables

In this scenario, linear correlation among random variables is considered. The power injections of generators 2 and 3 are assumed to follow the normal distribution with means being the original value and standard deviation being 10% of the means. The correlation between them is described using Pearson coefficient ρ. The aPC is combined with whitening transformation in this case and the collocation points are calculated by the k-means++ clustering method. The expansion orders of aPC and gPC methods are set to 3. The fault settings are the same as for scenario 1 and the benchmark is obtained based on MCS with 1000 samples. Due to the length limitation, only the results of rotor angle δ_1 of generator 1 are discussed below.

The detailed AAE results of δ_1, including the relative AAE of aPC compared to gPC, are presented in Table 3. The comparison of k-means++ clustering method and traditional root method is also presented in the table. First, the proposed aPC method also has better accuracy than the traditional gPC method. Also, note that with the growth of the Pearson coefficients, the improvement of aPC becomes more remarkable. This is because for gPC, the errors caused by correlation in (7) become larger, which makes the decorrelation process of greater importance. Moreover, the

reasons for the difference between Table 1 and 3 are, on the one hand, the input data of scenario 1 comes from the German Transmission System Operators which leads to larger distribution parameter fitting error. So the performance of aPC in scenario 1 is much better than that of gPC. On the other hand, in scenario 2, the distribution fitting error using gPC is relatively small, or even close to that of aPC, because the data is generated from normal distribution rather than practical measured data. The majority of errors for both methods are introduced by the increased number of random variables. In addition, gPC is also affected by errors caused by linear correlation. By comparing the collocation point selection methods, it is observed that the accuracy is very close. The main advantage of k-means++ clustering method is to avoid the problem of matrix singularity of the polynomial matrix H_φ in (5) when using root method. Using different root combinations could be time-consuming especially when the dimension of random variables and the expansion order are high.

The mean and standard deviation error of δ_1 when ρ=0.6 are plotted in Fig. 4.a and Fig. 4.b respectively. Fig. 4.a and Fig. 4.b show that aPC has better accuracy than gPC during the entire simulation period. Also, the effectiveness of whitening transformation is presented visually. Besides, it is observed again that as time increases, the average absolute mean and S.D. error become larger. The reason is the same as analyzed in Section 4.1. The AAE can be quantitatively verified in Table 3. The mean and error bar of δ_1 using the aPC method are plotted in red and grey respectively as shown in Fig. 4.c, which can provide operators with useful information to prevent the system from becoming unstable.

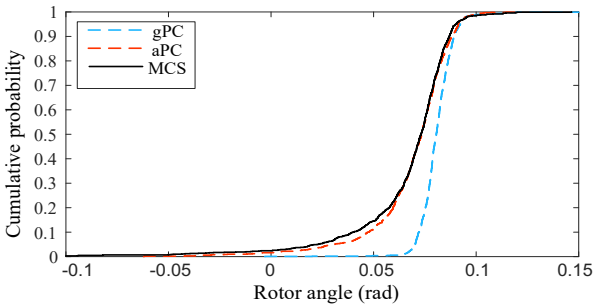

Fig. 5. Cumulative probability of δ_1 using MCS, gPC and aPC methods when ρ=0.6.

Fig. 5 shows the cumulative probability of δ_1 at t=7s. The density of MCS is directly obtained from the statistics of the time-domain simulation results while the cumulative probability of PCE-based methods is derived by substituting the original raw data into the established surrogate models (2). The results in Fig. 5 show that the curve of aPC algorithm is closer to the reference MCS result which indicates the original distribution is reconstructed better than gPC.

4.2. IEEE 300-Bus System

This second case study illustrates the adaptation of the proposed method in a larger system and research the performance of different types of nonlinear correlated uncertain inputs. To this aim we consider a modified model of the IEEE 300-bus system [49]. The practical data of PVs and wind farms with nonlinear correlation obtained from the National Renewable Energy Laboratory (NREL) [50] and GTSO is utilized in this case. The raw data is measured every 15 minutes for one month and the data size is 2976. Two PVs and two wind farms are connected to buses 20, 76, 124, and 125 to model the real volatile generation. 2 to 18 pairs of correlated Gaussian random loads are added and ρ is set to 0.4, respectively. The means of the active power consumption of the random loads are set equal to the original value and the standard deviations are σ = 3% of the means. The expansion order of PCE-based methods is set from 1 to 3, respectively. Hyperbolic truncation scheme is implemented to mitigate the curse of dimensionality. Since this algorithm is not a contribution of this paper, we do not introduce it further to save space. Details of the scheme can be found in [43]. All cross terms are excluded by adjusting the parameters of hyperbolic truncation scheme which effectively reduces the required number of simulations. For example, the polynomial terms of 3rd order PC-based methods decrease from 11480 to 118 which means only 118 simulations are required. Meanwhile, 2976 simulations

are performed for MCS. Admittedly, the accuracy of PC-based methods is decreased to some extent after truncation. However, this truncated scheme is implemented in both gPC and aPC methods which provides us a rigorous comparison of the differences in accuracy between them. The total simulation time is set to 10 s. A three-phase fault is imposed on bus 4 at t=1s and lasts for 0.1s by tripping bus 4.

Table 4 and Table 5 show the average absolute mean, standard deviation error comparison of the rotor angle δ_3 and rotor speed ω_3 of generator 3. The performance of gPC and aPC using different expansion order d in systems containing different numbers of random inputs N are tested. We have analyzed the overall performance on all machines and the performance across all machines is similar, thus only δ_3 and ω_3 are presented. The performance of aPC is still better than that of gPC overall. Moreover, with the order increase from 1 to 3, the accuracy of gPC is even worse, while the improvement of using aPC is significant or its accuracy is stable. The main reason is the inaccuracy of polynomial bases caused by the parameter fitting error of PDF and the correlation of inputs. The results once again demonstrate the importance of input decorrelation and data-driven construction of accurate polynomial bases in the aPC algorithm.

As the N is increased from 8 to 40, we can observe that the AAE of gPC decreases rapidly, while that of aPC remains stable. This phenomenon can be attributed to the error of the gPC basis accumulates as the number of random variables increases. In contrast, this problem is avoided in aPC due to its data-driven calculation of the optimal orthogonal basis. Moreover, the adverse influence of correlation is mitigated by Whitening transformation.

Compared with the results of the 9-bus system, the accuracy is decreased, which is the result of a variety of reasons, mainly including the increase in the number of random variables, the introduction of nonlinear correlation and the increase of the nonlinearity of the system model. Admittedly, the best way to tackle nonlinear correlation is by utilizing nonlinear decorrelation methods, such as Copula-based methods. This case is only to provide an alternative method if the copula-based method has an excessive approximation error caused by fitting the PDF of the raw data. Our future work includes investigating how to perform non-linear decorrelation directly based on the raw data.

Table 4
Average absolute mean error of the rotor angle and rotor speed

Method	$e_{\delta 3}$(rad×10^{-4})			$e_{\omega 3}$(rad/s×10^{-3})		
	N=8	N=24	N=40	N=8	N=24	N=40
gPC (d=1)	447.35	498.50	540.25	18.11	21.58	26.84
aPC (d=1)	7.99 (1.79%)	7.81 (1.57%)	8.24 (1.53%)	2.02 (11.15%)	2.15 (9.96%)	2.28 (8.49%)
gPC (d=2)	465.83	525.49	590.42	23.09	22.07	30.63
aPC (d=2)	8.21 (1.76%)	7.73 (1.47%)	8.07 (1.37%)	2.55 (11.04%)	2.37 (10.74%)	2.47 (8.06%)
gPC (d=3)	470.15	546.27	608.42	36.56	26.94	38.89
aPC (d=3)	8.20 (1.74%)	7.80 (1.43%)	8.11 (1.33%)	2.35 (6.43%)	2.27 (8.43%)	2.43 (6.25%)

Table 5
Average absolute standard deviation error of the rotor angle and rotor speed

Method	$e_{\delta 3}$(rad×10^{-3})			$e_{\omega 3}$(rad/s×10^{-3})		
	N=8	N=24	N=40	N=8	N=24	N=40
gPC (d=1)	3.54	7.90	9.74	6.63	14.24	25.51
aPC (d=1)	2.42 (68.36%)	4.95 (62.66%)	7.25 (74.44%)	6.05 (91.25%)	11.20 (78.65%)	14.80 (58.02%)
gPC (d=2)	6.59	12.73	17.32	10.57	21.85	39.19
aPC (d=2)	2.16 (32.78%)	3.34 (26.24%)	6.08 (35.10%)	5.50 (52.03%)	8.32 (38.08%)	11.08 (28.27%)
gPC (d=3)	11.24	20.58	46.85	17.36	37.87	56.52
aPC (d=3)	1.05 (9.34%)	3.96 (19.24%)	5.59 (11.93%)	3.29 (18.95%)	4.07 (10.75%)	5.73 (10.14%)

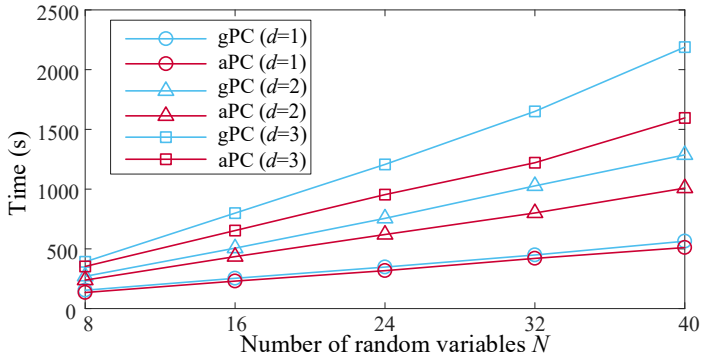

Fig. 6. Computational burden comparison of gPC and aPC

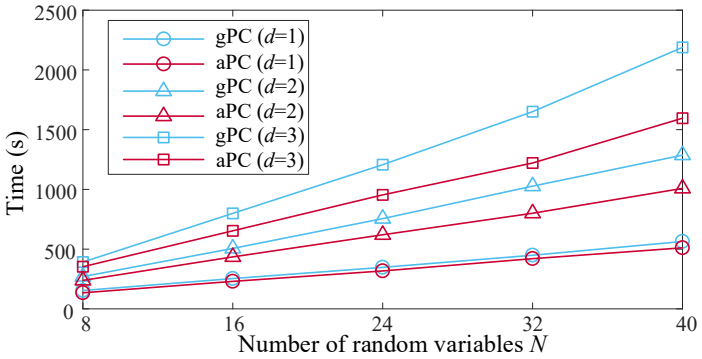

Fig. **6** shows the total computational burden t_{total} using different expansion orders d of gPC and aPC under different random variable numbers N. Since the same truncation scheme is implemented in both gPC and aPC, for a given N, the required number of simulations is same. It means the time consumption of solving procedure t_{sp} of both methods is very close. The difference between the two methods is mainly from the time consumption of preprocessing t_{pre} and postprocessing t_{post}. The reason why aPC is more timesaving than gPC in these two stages has been analyzed in Scenario 1 of Section 4.1. Besides, as d increases, the advantage of aPC in efficiency becomes more significant. Moreover, the growth rate of t_{total} is linear because the number of bases, required simulations, coefficients grow linearly with N under the setting of the truncation scheme.

The detailed computational burden when N=40 and d=3 is shown in Table 6. Results indicate that the PCE-based method can effectively improve efficiency compared to MCS. It is observed that aPC saves more time in the preprocessing and postprocessing stages than gPC. The computational burden difference becomes larger in this case compared to Scenario 1 in Section 4.1 due to the increased number of random variables and the increased simulation time. Moreover, the speed difference of the postprocessing stage is mainly because of the time-consuming integral operation of gPC in (7), while only several moments are needed to achieve the same target for aPC-based method (19). Note that since t_{post} is related linearly to the number of output variables to be studied, the efficiency of the PCE-based method is directly influenced. The advantage of the proposed method in computational efficiency is found in cases where limited number of outputs instead of complete system information is required. Note that when N=40 and d=3, the number of collocation points combinations of the traditional root method reaches 40^4=2,560,000. Since there is no theoretical basis for selecting collocation points that can avoid singularity, a large number of combination attempts could be required while k-means++ method can effectively avoid this issue.

Table 6
Computational burden of MCS, gPC, and aPC

Method	Time Components(s)			t_{total}(s)
	t_{pre}	t_{sp}	t_{post}	
MCS	-	35307.2	0.5	35307.7

gPC	408.2	1480.2	300.3	2188.7 (6.2%)
aPC	47.5	1478.7	69.6	1595.8 (4.5%)

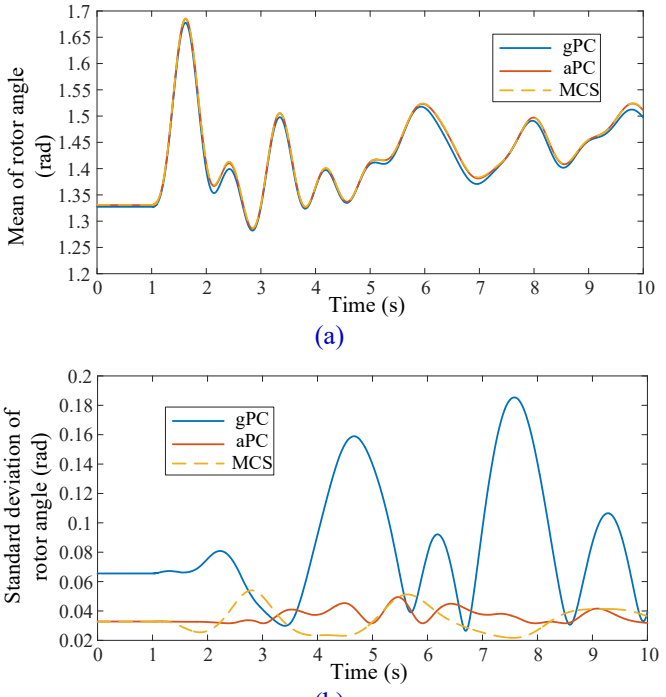

Fig.7. Mean and standard deviation of δ_3. (a) Mean of δ_3 using gPC, aPC, MCS methods. (b) Standard deviation of δ_1 using gPC, aPC, MCS methods.

Figure 7 shows the estimated mean and standard deviation of gPC, aPC and MCs when N=40 and d=3. The results in Fig. 7 show that the curves of aPC algorithm is closer to the reference MCS result which indicates the probabilistic features are more accurate than gPC.

5. Conclusions

The paper proposes an aPC-based framework combined with whitening transformation and k-means++ clustering to evaluate the propagation of uncertainties in dynamic power systems caused by RES. The proposed method is fully data-driven and free from any prior distribution assumptions or knowledge of the random inputs. The calculation speed is faster than the traditional gPC method because the integral operation in the preprocessing and postprocessing stages is effectively replaced by the moments of raw data. Moreover, whitening transformation is integrated to deal with the linear correlation which is very suitable to be combined with the aPC-based structure because the output data of whitening transformation can be directly utilized by aPC. It also has the capability to dealing with nonlinear correlation. In addition, the k-means++ clustering method is adopted to find the presentative collocation points which can effectively avoid the problem of matrix singularity when attempting different combinations of roots.

Future work will focus on exploring the data-driven nonlinear decorrelation method and the implementation of the PCE-based method in stochastic time-varying cases.

Appendix A

The moments' matrix M in Eq. (17) can be decomposed as:

$$M=\begin{bmatrix} H & B \\ C & D \end{bmatrix}$$

where

$$M=\begin{bmatrix} \mu_0 & \mu_1 & \cdots & \mu_k \\ \mu_1 & \mu_2 & \cdots & \mu_{k+1} \\ \vdots & \vdots & \vdots & \vdots \\ \mu_{k-1} & \mu_k & \cdots & \mu_{2k-1} \\ 0 & 0 & \cdots & 1 \end{bmatrix};\ H=\begin{bmatrix} \mu_0 & \mu_1 & \cdots & \mu_{k-1} \\ \mu_1 & \mu_2 & \cdots & \mu_k \\ \vdots & \vdots & \vdots & \vdots \\ \mu_{k-1} & \mu_k & \cdots & \mu_{2k-2} \end{bmatrix};\ B=\begin{bmatrix} \mu_k \\ \mu_{k+1} \\ \vdots \\ \mu_{2k-1} \end{bmatrix};\ C=\begin{bmatrix} 0 & \cdots & 0 \end{bmatrix};\ D=\begin{bmatrix} 1 \end{bmatrix}.$$

Since matrix D is invertible, based on the determinant rule for block matrix, the determinant of M can be transformed as follows:

$$|M|=|D|\left|H-BD^{-1}C\right|$$

From the above, we know that $|D|=1$ and $C=\begin{bmatrix} 0 & \cdots & 0 \end{bmatrix}$, so:

$$|M|=|H|$$

The properties of matrix H are presented in [38] that $|H|=0$ if and only if the distribution of random variable ξ has only k or fewer points of support, where k is the rank of H. The points of support of a probability distribution refer to the values for which the PDF or probability mass function (PMF) is nonzero. To discrete data set, it means the number of different values. This condition is equivalent to that $|H|\neq 0$ if and only if the number of support points of ξ is larger than k and all moments up to order $2k$-1 are finite.

Acknowledgements

This work is partly supported by the National Natural Science Foundation of China (NSFC) by funding C. Liu under project 52007133, the Sustainable Energy Authority of Ireland (SEAI) by funding F. Milano under project FRESLIPS, Grant No. RDD/00681, and the China Scholarship Council (CSC) by funding X. Li for 1 year study at the University College Dublin.

References

[1] Surinkaew T, Ngamroo I. Coordinated Robust Control of DFIG Wind Turbine and PSS for Stabilization of Power Oscillations Considering System Uncertainties. IEEE Transactions on Sustainable Energy. 2014;5:823-33.
[2] Liao X, Liu K, Zhang Y, Wang K, Qin L. Interval method for uncertain power flow analysis based on Taylor inclusion function. IET Generation, Transmission & Distribution. 2017;11:1270-8.
[3] Bilil H, Gharavi H. MMSE-based analytical estimator for uncertain power system with limited number of measurements. IEEE Trans Power Syst. 2018;33.
[4] Liu C, Lai Q. Power flow analytical solutions and multi-dimensional voltage stability boundary based on the multivariate quotient-difference method. CSEE Journal of Power and Energy Systems. 2021.
[5] Adeen M, Milano F. Modeling of Correlated Stochastic Processes for the Transient Stability Analysis of Power Systems. IEEE Transactions on Power Systems. 2021;36:4445-56.
[6] Qiu Y, Lin J, Chen X, Liu F, Song Y. Nonintrusive Uncertainty Quantification of Dynamic Power Systems Subject to Stochastic Excitations. IEEE Transactions on Power Systems. 2021;36:402-14.
[7] Cai J, Zhang Z, Wang M, Ge X. An improved sequential importance sampling method for reliability assessment of renewable power systems with energy storage. Energy Reports. 2023;9:1637-46.
[8] Yu H, Chung CY, Wong KP, Lee HW, Zhang JH. Probabilistic Load Flow Evaluation With Hybrid Latin Hypercube Sampling and Cholesky Decomposition. IEEE Transactions on Power Systems. 2009;24:661-7.
[9] Hajian M, Rosehart WD, Zareipour H. Probabilistic power flow by Monte Carlo simulation with Latin supercube

sampling. IEEE Transactions on Power Systems. 2012;28:1550-9.
[10] Xie Z, Ji T, Li M, Wu Q. Quasi-Monte Carlo based probabilistic optimal power flow considering the correlation of wind speeds using copula function. IEEE Transactions on Power Systems. 2017;33:2239-47.
[11] Dhople SV, Chen YC, DeVille L, Dominguez-Garcia AD. Analysis of Power System Dynamics Subject to Stochastic Power Injections. IEEE Transactions on Circuits and Systems I: Regular Papers. 2013;60:3341-53.
[12] Bu SQ, Du W, Wang HF. Probabilistic Analysis of Small-Signal Rotor Angle/Voltage Stability of Large-Scale AC/DC Power Systems as Affected by Grid-Connected Offshore Wind Generation. IEEE Transactions on Power Systems. 2013;28:3712-9.
[13] Yorino N, Abdillah M, Sasaki Y, Zoka Y. Robust power system security assessment under uncertainties using bi-level optimization. IEEE Transactions on Power Systems. 2017;33:352-62.
[14] Capitanescu F. Power System Flexibility Region Under Uncertainty With Respect to Congestion and Voltage Constraints. 2021 IEEE Madrid PowerTech: IEEE; 2021. p. 1-6.
[15] Choi H, Seiler PJ, Dhople SV. Propagating Uncertainty in Power-System DAE Models With Semidefinite Programming. IEEE Transactions on Power Systems. 2017;32:3146-56.
[16] Tian T, Kestelyn X, Thomas O, Amano H, Messina AR. An Accurate Third-Order Normal Form Approximation for Power System Nonlinear Analysis. IEEE Transactions on Power Systems. 2018;33:2128-39.
[17] Deng Z, Rotaru MD, Sykulski JK. Kriging assisted surrogate evolutionary computation to solve optimal power flow problems. IEEE Transactions on power systems. 2019;35:831-9.
[18] Xu Y, Netto M, Mili L. Propagating Parameter Uncertainty in Power System Nonlinear Dynamic Simulations Using a Koopman Operator-Based Surrogate Model. IEEE Transactions on Power Systems. 2022;37:3157-60.
[19] Zhang T, Sun M, Cremer JL, Zhang N, Strbac G, Kang C. A Confidence-Aware Machine Learning Framework for Dynamic Security Assessment. IEEE Transactions on Power Systems. 2021;36:3907-20.
[20] Li J, Xiu D. A generalized polynomial chaos based ensemble Kalman filter with high accuracy. Journal of Computational Physics. 2009;228:5454-69.
[21] Sun X, Tu Q, Chen J, Zhang C, Duan X. Probabilistic load flow calculation based on sparse polynomial chaos expansion. IET Generation, Transmission & Distribution. 2018;12:2735-44.
[22] Zeng X, Ghanem R. Projection pursuit adaptation on polynomial chaos expansions. Computer Methods in Applied Mechanics and Engineering. 2023;405.
[23] Wu H, Shen D, Xia B, Qiu Y, Zhou Y, Song Y. Parametric Problems in Power System Analysis: Recent Applications of Polynomial Approximation Based on Galerkin Method. Journal of Modern Power Systems and Clean Energy. 2021;9:1-12.
[24] Xia B, Wu H, Qiu Y, Lou B, Song Y. A Galerkin Method-Based Polynomial Approximation for Parametric Problems in Power System Transient Analysis. IEEE Transactions on Power Systems. 2019;34:1620-9.
[25] Al-Othman A, Irving M. A comparative study of two methods for uncertainty analysis in power system state estimation. IEEE Transactions on Power Systems. 2005;20:1181-2.
[26] Xiu D. Numerical methods for stochastic computations: a spectral method approach: Princeton university press; 2010.
[27] Xu Y, Mili L, Sandu A, Spakovsky MRv, Zhao J. Propagating Uncertainty in Power System Dynamic Simulations Using Polynomial Chaos. IEEE Transactions on Power Systems. 2019;34:338-48.
[28] Ye K, Zhao J, Duan N, Maldonado DA. Stochastic Power System Dynamic Simulation and Stability Assessment Considering Dynamics From Correlated Loads and PVs. IEEE Transactions on Industry Applications. 2022;58:7764-75.
[29] Fan M, Li Z, Ding T, Huang L, Dong F, Ren Z, et al. Uncertainty evaluation algorithm in power system dynamic analysis with correlated renewable energy sources. IEEE Transactions on Power Systems. 2021;36:5602-11.
[30] Xu Y, Dong ZY, Xu Z, Meng K, Wong KP. An intelligent dynamic security assessment framework for power systems with wind power. Ieee T Ind Inform. 2012;8:995-1003.
[31] Wu J, Zhang B, Li H, Li Z, Chen Y, Miao X. Statistical distribution for wind power forecast error and its application to determine optimal size of energy storage system. International Journal of Electrical Power & Energy Systems. 2014;55:100-7.
[32] Yang C, Du X, Xu D, Tang J, Lin X, Xie K, et al. Optimal bidding strategy of renewable-based virtual power plant in the day-ahead market. International Journal of Electrical Power & Energy Systems. 2023;144:108557.
[33] Wang Y, Chen T, Zou R, Song D, Zhang F, Zhang L. Ensemble probabilistic wind power forecasting with multi-scale features. Renewable Energy. 2022;201:734-51.

[34] Tan J, Wu Q, Zhang M, Wei W, Hatziargyriou N, Liu F, et al. Wind power scenario generation with non-separable spatio-temporal covariance function and fluctuation-based clustering. International Journal of Electrical Power & Energy Systems. 2021;130.
[35] Jia M, Shen C, Wang Z. A distributed incremental update scheme for probability distribution of wind power forecast error. International Journal of Electrical Power & Energy Systems. 2020;121.
[36] Jónsdóttir GM, Milano F. Data-based continuous wind speed models with arbitrary probability distribution and autocorrelation. Renewable Energy. 2019;143:368-76.
[37] Wang G, Xin H, Wu D, Ju P, Jiang X. Data-Driven Arbitrary Polynomial Chaos-Based Probabilistic Load Flow Considering Correlated Uncertainties. IEEE Transactions on Power Systems. 2019;34:3274-6.
[38] Oladyshkin S, Nowak W. Data-driven uncertainty quantification using the arbitrary polynomial chaos expansion. Reliability Engineering & System Safety. 2012;106:179-90.
[39] Conrad PR, Marzouk YM. Adaptive Smolyak pseudospectral approximations. SIAM Journal on Scientific Computing. 2013;35:A2643-A70.
[40] Xiong H, Wu J, Chen J. K-means clustering versus validation measures: a data distribution perspective. Proceedings of the 12th ACM SIGKDD international conference on Knowledge discovery and data mining2006. p. 779-84.
[41] Rahman S. A polynomial chaos expansion in dependent random variables. Journal of Mathematical Analysis and Applications. 2018;464:749-75.
[42] Kundur PS, Malik OP. Power system stability and control: McGraw-Hill Education; 2022.
[43] Marelli S, Sudret B. UQLab: A Framework for Uncertainty Quantification in Matlab. Vulnerability, Uncertainty, and Risk2014. p. 2554-63.
[44] Zimmerman RD, Murillo-Sánchez CE, Thomas RJ. MATPOWER: Steady-state operations, planning, and analysis tools for power systems research and education. IEEE Transactions on power systems. 2010;26:12-9.
[45] Abdulrahman I. MATLAB-Based Programs for Power System Dynamic Analysis. IEEE Open Access Journal of Power and Energy. 2020;7:59-69.
[46] Wind power generation from four German energy companies (50 Hertz, Amprion, TenneT TSO and TransnetBW). https://www.kaggle.com/datasets/jorgesandoval/wind-power-generation
[47] Wan X, Karniadakis GE. An adaptive multi-element generalized polynomial chaos method for stochastic differential equations. Journal of Computational Physics. 2005;209:617-42.
[48] Gerritsma M, Van der Steen J-B, Vos P, Karniadakis G. Time-dependent generalized polynomial chaos. Journal of Computational Physics. 2010;229:8333-63.
[49] Power System Test Case Archive. http://labs.ece.uw.edu/pstca/
[50] NREL Western Wind Data Set. https://www.nrel.gov/grid/western-wind-data.html